J|A|C|S
ARTICLES
Published on Web 03/28/2002

On the Effect of Covalently Appended Quinolones on Termini of DNA Duplexes

Jennifer Tuma,[‡] William H. Connors,[‡,§] David H. Stitelman,[§] and Clemens Richert*[,‡,§]

Contribution from the Departments of Chemistry, University of Constance, Fach M 709, D-78457 Konstanz, Germany, and Tufts University, Medford, Massachusetts 02155

Received November 8, 2001

Abstract: Quinolones are gyrase inhibitors that are widely used as antibiotics in the clinic. When covalently attached to oligonucleotides as 5′-acylamido substituents, quinolones were found to stabilize duplexes of oligonucleotides against thermal denaturation. For short duplexes, such as qu-T*GCGCA, where qu is a quinolone residue and T* is a 5′-amino-5′-deoxythymidine residue, an increase in the UV melting point of up to 27.8 °C was measured. The stabilizing effect was demonstrated for all quinolones tested, namely nalidixic acid, oxolinic acid, pipemidic acid, cinoxacin, norfloxacin, and ofloxacin. The three-dimensional structure of (oa-T*GCGCA)$_2$, where oa is an oxolinic acid residue, was solved by two-dimensional NMR spectroscopy and restrained molecular dynamics. In this complex, the oxolinic acid residues disrupt the terminal T1:A6 base pairs and stack on the G2:C5 base pairs. The displaced adenosine residues bind in the minor groove of the core duplex, while the thymidine residues pack against the oxolinic acid residues. The "molecular cap" thus formed fits tightly on the G:C base pairs, resulting in increased base-pairing fidelity, as demonstrated in UV melting experiments with the sequence oa-T*GGTTGAC and target strands containing a mismatched nucleobase. The structure of the "molecular cap" with its disrupted terminal base pair may also be helpful for modeling how quinolones block re-ligation of DNA strands in the active site of gyrases.

Introduction

Quinolones have been used as antimicrobial agents in the clinic for many years. These synthetic antibiotics target both gyrases (type II topoisomerases) and topoisomerase IV.[1] They inhibit the negative supercoiling introduced to bacterial DNA by the gyrases. Eukaryotic cells, on the other hand, lack DNA gyrases and solve topological problems for genomic DNA through other enzymes. While quinolones such as nalidixic acid (Neggram) are currently of minor significance, being mainly used for treating urinary tract infections, the 6-fluoroquinolones, most notably ciprofloxacin (Ciprobay) and ofloxacin (Floxin) have broad antibacterial activity and are used widely to treat bacterial infections, including those with anthrax.

It has been known for some time that quinolones can bind to DNA[2] and to gyrase−DNA complexes,[3] but it is the binding to the DNA−gyrase complexes that correlates with inhibition.[4] Quinolones interrupt the reunion of genomic DNA that occurs at the end of the cleavage ligation cycle in the active site of the gyrases. The structure of the "breakage−reunion" domain of a type-II DNA topoisomerase from bacteria has been solved,[5] albeit without substrate or inhibitors. Mechanisms for the inhibition of the gyrase reaction by quinolones have been proposed,[6,7] partly based on docking the gyrases with duplex DNA, but the molecular details of how the quinolones interfere with the gyrase reaction are not completely clear.

While screening libraries of acylamidooligonucleotides in spectrometrically monitored selection experiments (SMOSE), we became aware of the stabilizing effect of quinolone residues appended covalently to the 5′-terminus of one or both strands of a duplex.[8] The effect was first discovered for an oxolinic acid residue in the context of the duplex (oa-T*GCGCA)$_2$ (**1oa**)$_2$, where T* denotes a 5′-amino-5′-deoxythymidine residue and oa an oxolinic acid residue (Figure 1). Recently, we also noted the duplex-stabilizing effects of five other 5′-appended quinolone residues when working with DNA duplexes terminat-

* To whom correspondence should be addressed. Telephone: 49 (0)-7531 88-4572. Fax: 49 (0)7531 88-4573. E-mail: Clemens.Richert@uni-konstanz.de.
‡ University of Constance.
§ Tufts University.

(1) Drlica, K.; Zhao, X. *Microbiol. Mol. Biol. Rev.* **1997**, *61*, 377−392.
(2) (a) Shen, L. L.; Pernet, A. G. *Proc. Natl. Acad. Sci. U.S.A.* **1985**, *82*, 307−311. (b) Shen, L. L.; Baranowski, J.; Pernet, A. G. *Biochemistry* **1989**, *28*, 3879−3885. (c) Hiasa, H.; Shea, M. E. *J. Biol. Chem.* **2000**, *275*, 34780−34786.
(3) (a) Critchlow, S. E.; Maxwell, A. *Biochemistry* **1996**, *35*, 7387−7393. (b) Kulkarni, T.; Mitscher, L. A.; Shen, L. L.; Telikepalli, H.; Wei, D. *Bioorg. Med. Chem. Lett.* **2997**, *7*, 1097−1100.
(4) (a) Shen, L. L.; Kohlbrenner, W. E.; Weigl, D.; Baranowski, J. *J. Biol. Chem.* **1989**, *264*, 2973−2978. (b) Yoshida, H.; Nakamura, H.; Bogaki, M.; Ito, H.; Kojima, T.; Hattori, H.; Nakamura, S. *Antimicrob. Agents Chemother.* **1993**, *37*, 839−845.
(5) Morais Cabral, J. H.; Jackson, A. P.; Smith, C. V.; Shikotra, N.; Maxwell, A.; Liddington, R. C. *Nature* **1997**, *388*, 903−906.
(6) Shen, L. L.; Tanaka, S. K.; Chu, D. T. W. *Curr. Pharm. Des.* **1997**, *3*, 169−176.
(7) Heddle, J. G.; Barnard, F. M.; Wentzell, L. M.; Maxwell, A. *Nucleosides Nucleotides Nucleic Acids* **2000**, *19*, 1249−1264.
(8) Altman, R. K.; Schwope, I.; Sarracino, D. A.; Tetzlaff, C. N.; Bleczinski, C. F.; Richert, C. *J. Comb. Chem.* **1999**, *1*, 493−508.

10.1021/ja0125117 CCC: $22.00

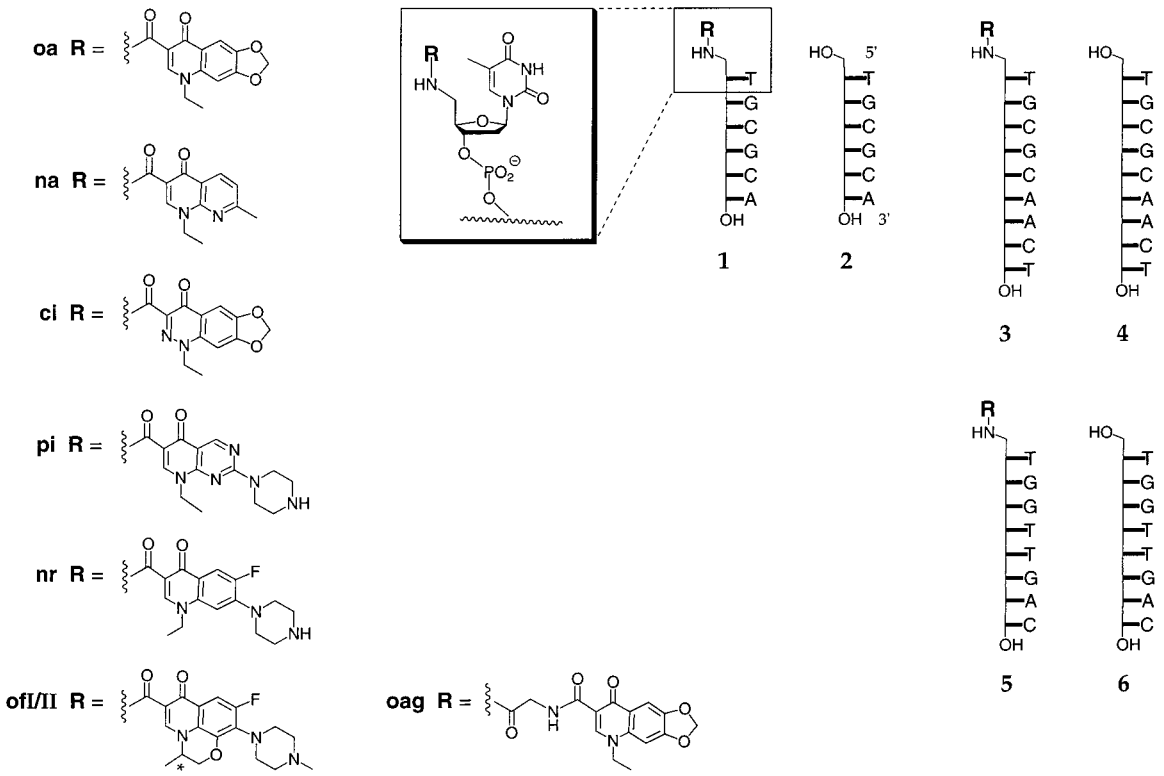

Figure 1. Sequences of oligonucleotides and structural formulae of quinolone residues employed.

ing in C:G base pairs.[9] Further, a nalidixic acid residue appended as 2′-acylamido group to a 3′-terminal uridine residue was found to increase the UV melting point of oligonucleotide duplexes.[10] Finally, residues of nalidixic acid, when bonded to the α- and ϵ-amino groups of the terminal residues of small lysine dendrimers, were identified as moieties that decelerate the enzymatic degradation of oligonucleotides.[11]

Thus far, the structural basis of the effect of quinolones on DNA duplexes has been unknown. Here we report data that provide direct and indirect evidence for a duplex-stabilizing, but base-pair-disrupting effect of oxolinic acid residues interacting with DNA duplexes. A detailed UV melting study showed strong duplex-stabilizing effects for quinolones 5′-bonded to oligonucleotides, but no base selectivity for the terminal nucleotide of the target strand. On the other hand, exquisite base-pairing fidelity was found at the penultimate position of the duplexes of oxolinic acid-bearing sequence oa-T*GGTTGAC. Other quinolones, when appended to T*GCGCA, also exhibited substantial duplex-stabilizing effects. The three-dimensional structure of duplex (oa-T*GCGCA)$_2$, obtained via two-dimensional NMR and restrained molecular dynamics, showed a core duplex and termini without T:A base pairs.

Results

Starting from (oa-T*GCGCA)$_2$, (**1oa**)$_2$, where oa denotes the oxolinic acid residue, the compound identified as forming an unusually stable duplex in the earlier combinatorial work,[8] the structural requirements for duplex stabilization were probed. This involved synthesizing derivatives of **1oa** (Figure 1) and determining the stability of their duplexes in UV melting experiments. First, acylamido derivatives of self-complementary sequence 5′-T*GCGCA-3′ with quinolone residues other than oxolinic acid were prepared, and their UV melting points (T_m's) at 10, 150, and 1000 mM salt concentrations were determined (Table 1). The duplex of oxolinic acid-bearing **1oa** showed melting points 25.7−26.9 °C higher than those of control duplex (**2**)$_2$ and greater hyperchromicity (Figure 2). Duplex (**1na**)$_2$, with nalidixic acid residues as 5′-caps, gave T_m increases of 20.1−21.1 °C. The melting points of (**1ci**)$_2$, whose quinolone appendages are cinoxacin residues, were similar to those of (**1oa**)$_2$, to which it is isoelectronic. When a melting curve was measured at 360 nm, where only the cinoxacin moiety absorbs, a melting point almost identical to that observed at 260 nm was measured (56.4 versus 57.5 °C at 1 M salt concentration). For pipemidic acid-capped (**1pi**)$_2$, with its nonannulated piperazine rings, the highest melting point increase over control (**2**)$_2$ of all compounds tested was measured (+27.8 °C at 10 mM salt concentration). This effect dwindled to +18.6 °C at high salt concentration, where ion pairs are less stable. Fluoroquinolone norfloxacin, when appended as a 5′-residue to give **1nr**, did not produce higher duplex melting points than **1pi**, nor was the tetracyclic quinolone ofloxacin (**1of**) more effective as a cap for the duplex. Since ofloxacin was available as a racemic mixture, two diastereomers of **1of** were obtained, which were enriched during HPLC and named **1of**(**I**) for the faster-eluting diastereomer and **1of**(**II**) for the slower-eluting one. The duplex-stabilizing effect of either isomer was weaker than that of all other quinolones tested, except for nalidixic acid, which was less stabilizing at 10 mM salt concentration. Still, a melting point increase of 12.7 °C was measured for the ofloxacin

(9) Mokhir, A. A.; Tetzlaff, C. N.; Herzberger, S.; Mosbacher, A.; Richert, C. *J. Comb. Chem.* **2001**, *3*, 374−386.
(10) Kryatova, O. P.; Connors, W. H.; Bleczinski, C. F.; Mokhir, A. A.; Richert, C. *Org. Lett.* **2001**, *3*, 987−990.
(11) Sarracino, D. A.; Richert, C., *Bioorg. Med. Chem. Lett.* **2001**, *11*, 1733−1736.

Table 1. UV Melting Points, Hyperchromicities, and Free Energies of Dissociation of Duplexes Formed by Self-Complementary Sequences

duplex[a]	T_m at [salt] (°C)[b] 10 mM	150 mM	1 M	hyperchromicity (%)[c]	$\Delta G°$ (kcal/mol)[d]
$(TGCGCA)_2$ $(\mathbf{2})_2$	21.0 ± 1.1	31.6 ± 1.7	33.5 ± 0.5	10.6 ± 2.7	6.9
$(oa\text{-}T^*GCGCA)_2$ $(\mathbf{1oa})_2$	47.0 ± 0.5	58.5 ± 1.8	59.2 ± 0.3	13.3 ± 0.5	11.2
$(na\text{-}T^*GCGCA)_2$ $(\mathbf{1na})_2$	41.1 ± 0.2	52.7 ± 0.7	54.1 ± 0.7	13.3 ± 0.8	10.3
$(ci\text{-}T^*GCGCA)_2$ $(\mathbf{1ci})_2$	45.8 ± 0.4	56.8 ± 0.4	57.5 ± 1.1	9.1 ± 0.2	11.1
$(pi\text{-}T^*GCGCA)_2$ $(\mathbf{1pi})_2$	48.8 ± 0.7	55.4 ± 0.7	52.1 ± 0.7	7.9 ± 0.7	10.6
$(nr\text{-}T^*GCGCA)_2$ $(\mathbf{1nr})_2$	46.0 ± 0.5	52.8 ± 0.5	49.5 ± 0.5	6.8 ± 0.5	10.4
$(ofI\text{-}T^*GCGCA)_2$ $(\mathbf{1ofI})_2$[e]	45.8 ± 0.3	50.9 ± 1.3	49.5 ± 0.8	11.7 ± 0.4	10.3
$(ofII\text{-}T^*GCGCA)_2$ $(\mathbf{1ofII})_2$[e]	43.3 ± 0.4	48.6 ± 1.3	46.2 ± 1.4	9.3 ± 1.8	9.6
$(oa\text{-}Gly\text{-}T^*GCGCA)_2$ $(\mathbf{1oag})_2$	33.8 ± 0.2	44.2 ± 0.2	46.4 ± 0.5	17.5 ± 0.9	9.3
$(TGCGCAACT)_2$ $(\mathbf{4})_2$	32.1 ± 0.7	26.8 ± 0.7	32.4 ± 0.5	11.5 ± 2.6	(8.5)[f]
$(oa\text{-}T^*GCGCAACT)_2$ $(\mathbf{3oa})_2$	52.4 ± 0.8	54.6 ± 0.5	58.4 ± 1.5	13.1 ± 1.4	10.2

[a] Sequences are given 5′- to 3′-terminus; T* denotes a 5′-amino-5′-deoxythymidine residue. [b] Average from at least three melting curves ± one standard deviation (SD) at 3.1 ± 0.3 μM strand concentration. Salt concentrations are those of the ammonium acetate buffer, pH 7. [c] Hyperchromicity at 260 nm and 150 mM salt concentration upon duplex dissociation (average of four melting curves ± SD). [d] Derived from fits to the UV melting data at 150 mM salt concentration, using the program Meltwin.[43] See Table S4 for enthalpy and entropy values. [e] I and II denote earlier and later eluting diastereomers of the ofloxacin−DNA hybrid. [f] Low-temperature baseline not suitable for accurate fitting.

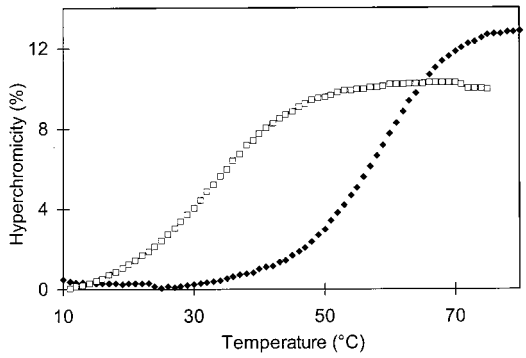

Figure 2. UV melting curves of control duplex $(\mathbf{2})_2$ (open squares) and quinolone-bearing $(\mathbf{1oa})_2$ (solid squares) at 260 nm in 1 M NH_4OAc. See Table 1 for melting points.

appendage, even in the least favorable case (isomer **II**, 1 M salt concentration).

On the next stage of the structural probing, changes were made in the non-quinolone portion of duplex $(\mathbf{1oa})_2$. An intervening glycine residue was inserted between the DNA and the oxolinic acid residue (derivative **1oag**). As a result, the duplex-stabilizing effect of the quinolone was roughly halved, although still at a respectable +12.6−12.9 °C (Table 1). Addition of three nucleotide residues to the 3′-terminus of the hexamer sequence TGCGCA gave compounds **4** and **3oa**, whose 3′-overhang was envisioned to present a possible block to the stabilizing effect of the oxolinic acid. Little blocking was observed, however, with ΔT_m's of +20.3−27.8 °C between the melting points of $(\mathbf{3oa})_2$ and $(\mathbf{4})_2$. In this study, control duplex $(\mathbf{4})_2$ gave an unusual salt dependence of its melting point when proceeding from 10 to 150 mM salt concentration. The decrease was reproducible, and we currently do not have an explanation for the effect. As expected, the melting point of $(\mathbf{4})_2$ at 1 M salt concentration was close to that of $(\mathbf{2})_2$. At this salt concentration, $(\mathbf{2})_2$ melted 26 °C lower than $(\mathbf{3oa})_2$. Together, these data show that the duplex-stabilizing effect observed for $(\mathbf{1oa})_2$ does depend on the nature of the quinolone, suffers when a longer linker is used, but is largely unaffected by a trinucleotide overhang at the 3′-terminus of the target strand.

A study with H-Lys(oa)-T*GGTTGAC, where an oxolinic acid residue is appended via the ϵ-amino group of a lysine residue, and GTCAACCA as target strand gave melting point increases of 5.4−6.8 °C for the modified duplexes over control duplex **6**:GTCAACCA (data not shown),[12] demonstrating that a fair portion of the stabilizing effect of the quinolone is experienced, even if the quinolone is appended via a long and floppy linker (longer than the glycine residue in **1oag**). This was also confirmed for duplex oa-Lys-T*GCGCG, whose strong melting hyperchromicity (16.2%) and substantial melting point increase over $(TGCGCG)_2$ and $(\mathbf{2})_2$ (+17.1 and +13.6 °C at 1 M salt concentration) were greater than those for $(\mathbf{1oag})_2$, despite the T:G mismatches at the termini.[13] Bis-quinolone−DNA hybrids of the sequence H-Lys(oa)-$(Gly)_n$-Lys(oa)-T*GGTTGAC, with $n = 0-2$, in duplex with GTCAACCA gave melting point increases of 3.9−5.8 °C relative to the control sequence, indicating that a second quinolone does not stabilize the duplex further.[12]

The sequence dependence of the duplex stabilization was probed next. For this, non-self-complementary octamer 5′-TGGTTGAC-3′, either with (**5**) or without (**6**) quinolone appendages, was presented to target strands with a mismatched nucleobase, and the melting point of the resulting duplexes were determined (Table 2). At all three salt concentrations employed, little destabilization was found for duplexes of **5oa** with a target octamer containing a mismatched nucleobase at its 3′-terminus. For control duplexes **6**:GTCAACC**X**, where **X** is the mismatched nucleotide, the melting point depression was only slightly greater, though, probably because of limited base contact due to wobbling and fraying at the terminus. In duplexes between oa-Lys-T*GGTTGAC, where the oxolinic acid residue is linked to the DNA via a lysine residue and target strands GTCAACC**G** and GTCAACC**A**, the melting point depression for the mismatch (or lack thereof) was virtually identical to that observed with directly linked hybrid **5oa** (Table S5, Supporting Information). When a mismatch was introduced at the penultimate position of the target strand, however, more significant drops in the melting point were observed for the duplexes with **5oa** (ΔT_m's from −15.7 to −20.6 °C), whereas control duplexes with **6** tolerated these mismatches better (ΔT_m from −10.1 to −12.3 °C). Further, it was noted that the drops in hyperchromicity accompanying duplex melting were greater for mismatched duplexes of **5oa** than for the corresponding duplexes formed with **6** (Table 2).

(12) Bleczinski, C. F., Ph.D. Thesis, Tufts University, 2000.
(13) Altman, R. K.; Richert, C. Unpublished results.

Table 2. UV Melting Points of Duplexes of **5oa** or **6** and a Target Strand with or without a Mismatched Nucleobase at 1.3 ± 0.3 μM Strand Concentration

[salt][a]	oligonucleotide[b]	target strand[b]	T_m (°C)[c]	T_m depression to match	hyperch. (%)[d]
10 mM[e]					
	oa-T*GGTTGAC	GTCAACCA**A**	20.3 ± 0.9	−.−	18.3
		GTCAACC**C**	19.6 ± 0.8	−0.7	17.6
		GTCAACC**G**	20.9 ± 0.9	+0.6	17.8
		GTCAACC**T**	18.8 ± 1.0	−1.5	18.7
	TGGTTGAC	GTCAACCA**A**	15.3 ± 1.0	−.−	13.8
		GTCAACC**C**	<15	<−0.3	.[f]
		GTCAACC**G**	<15	<−0.3	.[f]
		GTCAACC**T**	<15	<−0.3	.[f]
150 mM					
	oa-T*GGTTGAC	GTCAACCA**A**	38.0[g]	−.−	23.3
		GTCAACC**C**	37.7[g]	−0.3	18.5
		GTCAACC**G**	37.9[g]	−0.1	19.3
		GTCAACC**T**	36.3[g]	−1.7	20.1
		GTCAAC**A**A	17.4[g]	−20.6	.[f]
		GTCAAC**T**A	20.0 ± 1.3	−18.0	14.2
		GTCAAC**G**A	18.5 ± 0.9	−19.5	14.4
	TGGTTGAC	GTCAACCA**A**	29.8 ± 0.5	−.−	17.7
		GTCAACC**C**	28.0 ± 0.6	−1.8	17.1
		GTCAACC**G**	28.6 ± 0.8	−1.2	15.2
		GTCAACC**T**	28.9 ± 0.6	−0.9	15.6
		GTCAAC**A**A	17.5 ± 0.3	−12.3	16.3
		GTCAAC**T**A	19.7 ± 0.7	−10.1	17.0
		GTCAAC**G**A	17.5 ±0.8	−12.3	14.8
1 M					
	oa-T*GGTTGAC	GTCAACCA**A**	43.8 ± 0.5	−.−	20.7
		GTCAACC**C**	43.6 ± 0.8	−0.2	19.6
		GTCAACC**G**	44.3 ± 0.4	+0.5	19.5
		GTCAACC**T**	42.8 ± 0.5	−1.0	21.2
		GTCAAC**A**A	26.2 ± 0.4	−17.6	16.1
		GTCAAC**T**A	28.1 ± 1.3	−15.7	14.5
		GTCAAC**G**A	25.6 ± 1.2	−18.2	15.8
	TGGTTGAC	GTCAACCA**A**	36.1 ± 0.3	−.−	18.5
		GTCAACC**C**	34.0 ± 0.7	−2.1	17.9
		GTCAACC**G**	34.7 ± 0.5	−1.4	16.8
		GTCAACC**T**	34.2 ± 0.5	−1.9	18.1
		GTCAAC**A**A	24.2 ± 0.5	−11.9	17.8
		GTCAAC**T**A	25.9 ± 0.2	−10.2	17.9
		GTCAAC**G**A	24.2 ±1.5	−11.9	17.7

[a] Concentration of ammonium acetate buffer, pH 7. [b] Sequences are given 5′- to 3′-terminus; T* denotes a 5′-amino-5′-deoxythymidine residue. [c] Average of four melting points ± SD, except where indicated otherwise. [d] Average of hyperchromicity at 260 nm upon duplex dissociation. [e] All melting points of **5oa** and **6** with targets containing a mismatched base at the penultimate position were <15 °C at this salt concentration. [f] Baseline for hyperchromicity determination not established unambiguously. [g] Average of two melting points.

Similar trends were observed when target strands lacking terminal nucleotides were presented to **5oa** and **6** (Table 3). Deleting the 3′-terminal nucleotide of GTCAACCA to give heptamer GTCAACC led to small melting point decreases for duplexes with both probes. Deleting the penultimate deoxycytidine phosphate residue, however, again led to a more pronounced destabilization of the duplex with **5oa** (ΔT_m approximately −21 °C) than of the duplex with **6** (ΔT_m −9.7−10.8 °C). The duplex with hexamer GTCAAC was, in fact, less stable in the presence of the oxolinic acid residue than in its absence (melting points 3.9 and 3.4 °C lower than those of the control). Furthermore, the hyperchromicity upon duplex formation dropped more substantially when the penultimate base pair was deleted or disrupted by a mismatch when **5oa** was the probe strand than when **6** was the probe strand. Since the quinolone does contribute approximately one-third to the extinction of **5oa** at 260 nm, these data indicated that the oxolinic acid requires the presence of the penultimate base pair for its interactions with the duplex.

A final UV melting study with heptamer target strands was performed at 3 μM strand concentration to ensure that melting points were high enough for duplexes containing a mismatch (Table 4). At 10 mM salt concentration, T_m's were still too low to determine the melting point decreases for a G:T wobble base pair instead of a G:C base pair at the terminus of the octamer: heptamer duplex. At 150 and 1000 mM salt concentration, however, ΔT_m's could be measured for all four duplexes. Again, mismatch discrimination in the duplex with **5oa** was excellent, with melting point decreases of −18.1 and −17.2 °C for the mismatch. The corresponding ΔT_m for unmodified control strand **6** with GTCAACC or GTCAACT as matched and mismatched targets, respectively, was −9.5 °C at both salt concentrations. Since the melting point decreases for the wobble base pair were similar to those observed for the octamer/octamer duplex (Table 2), it is safe to state that residue A8 of the target strand is not critical for the duplex-stabilizing effect of the oxolinic acid residue. The G2:C5 base pair of $(\mathbf{1oa})_2$, on the other hand, is critically important for the quinolone to exert its effect.

Because at physiological or near-physiological ionic strength, the oxolinic acid residue gave the greatest stabilization among the quinolones tested, it was decided to subject $(\mathbf{1oa})_2$ to NMR-based structure elucidation. Samples were prepared on a 10 μmol scale and one- and two-dimensional spectra were acquired in D_2O and H_2O/D_2O (85:15), both under salt-free conditions and in solutions with 10 mM phosphate buffer, pH 7.0, and 150 mM NaCl. Conventional assignment strategies[14] were successful for the DNA portion of the quinolone−DNA hybrid. Deletion analysis together with NOESY cross-peak correlations between the ethyl side chain or the formacetal methylene group and the aromatic protons of the oxolinic acid allowed assignment of the resonances of the quinolone residue. NOESY cross-peaks in spectra acquired at 300 ms mixing time, together with coupling constants and resonances of nucleobase involved in hydrogen bonding yielded constraints for molecular dynamics (Table 5). These restrained molecular dynamics calculations were performed with CNS.[15] The torsion angle molecular dynamics approach[15b] produced the highest yield of duplex structures. Since early attempts to produce violation free structure with six base pairs were unsuccessful, low field resonances for a fifth/sixth base pair were absent, and the melting experiments with mismatched strands (Table 2) had shown no compliance with the Watson−Crick pairing rules for the terminal nucleotides, base-pairing constraints were applied only for the central four nucleotides of each strand.

Key NOESY cross-peaks between the oxolinic acid residue and the penultimate cytidine residue of the opposing strand located the oxolinic acid over the G2:C5 base pair (Figure S14, Supporting Information). Cross-peaks between protons of A6 and C5 put the 3′-terminal residue in the minor groove of the core duplex. The position of residue T1, which like A6 does not engage in base pairing, had to be established in a detailed refinement study, aimed at optimal agreement between experimental and back-calculated NOESY spectra. This refinement

(14) (a) Scheek, R. M.; Boelens, R.; Russo, N.; van Boom, J. H.; Kaptein, R. *Biochemistry* **1984**, *23*, 1371−1376. (b) Feigon, J.; Leupin, W.; Denny, W. A.; Kearns, D. R. *Biochemistry* **1983**, *22*, 5943−5951. (c) Patel, D. J.; Shapiro, L.; Hare, D. *J. Biol. Chem.* **1986**, *261*, 1223−1229.

(15) (a) Brünger, A. T.; Adams, P. D.; Clore, G. M.; DeLano, W. L.; Gros, P.; Grosse-Kunstleve, R. W.; Jiang, J.-S.; Kuszewski, J.; Nilges, N.; Pannu, N. S.; Read, R. J.; Rice, L. M.; Simonson, T.; Warren, G. L. *Acta Crystallogr.* **1998**, *D54*, 905−921. (b) Stein, E. G., Rice, L. M., and Brünger, A. T. *J. Magn. Reson. Ser. B* **1997**, *124*, 154−164.

Table 3. UV Melting Points of Duplexes of Octamers **5** and **6** with Heptamer or Hexamer Target Strands at 1.3 ± 0.3 Strand Concentration

[salt][a]	oligonucleotide[b]	target strand[b]	T_m (°C)[c]	drop per nucleotide[d]	hyperchromicity (%)[e]
10 mM					
	oa-T*GGTTGAC	GTCAACC	17.8 ± 0.4	2.5	18.0
		GTCAAC	<15	>2.8	–
	TGGTTGAC	GTCAACC	<15	>0.3	–
		GTCAAC	<15	–	–
150 mM					
	oa-T*GGTTGAC	GTCAACC	34.1 ±0.4	3.9	21.9
		GTCAAC	13.2 ± 1.3	20.9	14.6
	TGGTTGAC	GTCAACC	26.8 ± 1.0	3.0	18.9
		GTCAAC	17.1 ± 0.5	9.7	19.1
1 M					
	oa-T*GGTTGAC	GTCAACC	39.4 ± 0.5	4.4	21.0
		GTCAAC	18.3 ± 0.6	21.1	15.3
	TGGTTGAC	GTCAACC	32.5 ± 0.6	3.6	19.8
		GTCAAC	21.7 ± 0.4	10.8	20.5

[a] Concentration of ammonium acetate buffer, pH 7. [b] Sequences are given 5′- to 3′-terminus; T* denotes a 5′-amino-5′-deoxythymidine residue. [c] Average of four melting points ± SD, except where indicated otherwise. [d] Decrease of the melting point compared to the duplex with a target strand one nucleotide longer. (Compare Table 2 for melting points of octamer/octamer duplexes). [e] Average hyperchromicity at 260 nm upon duplex dissociation.

Table 4. UV Melting Points of Duplexes of **5** or **6** and Heptamer Target Strands with or without a Mismatched Nucleobase at 3.0 ± 0.4 μM Strand Concentration

[salt][a]	oligonucleotide[b]	target strand[b]	T_m (°C)[c]	T_m depression to match	hyperchromicity (%)[d]
10 mM					
	oa-T*GGTTGAC	GTCAAC**C**	21.3 ± 0.5	–.–	19.7
		GTCAAC**T**	<15	<–6.3	–
	TGGTTGAC	GTCAAC**C**	15.0 ± 0.3	–.–	14.9
		GTCAAC**T**	<15	–.–	–
150 mM					
	oa-T*GGTTGAC	GTCAAC**C**	38.4 ± 0.4	–.–	20.3
		GTCAAC**T**	20.3 ± 0.8	–18.1	15.2
	TGGTTGAC	GTCAAC**C**	29.7 ±1.2	–.–	16.5
		GTCAAC**T**	20.2 ±0.8	–9.5	16.2
1 M					
	oa-T*GGTTGAC	GTCAAC**C**	43.9 ± 0.3	–.–	17.3
		GTCAAC**T**	26.7 ± 0.8	–17.2	12.9
	TGGTTGAC	GTCAAC**C**	35.5 ± 1.2	–.–	16.2
		GTCAAC**T**	26.0 ± 1.2	–9.5	13.8

[a] Concentration of ammonium acetate buffer, pH 7. [b] Sequences are given 5′- to 3′-terminus; T* denotes a 5′-amino-5′-deoxythymidine residue. [c] Average of four melting points ± SD, except where indicated otherwise. [d] Average hyperchromicity at 260 nm upon duplex dissociation.

Table 5. Statistical Data on the Structure of (**1oa**)$_2$ as Determined by Restrained Molecular Dynamics

constraints	
NOE-based total	124
interresidue	72
intraresidue	52
dihedral angle constraints	26
hydrogen bond constraints	12
base pair planarity constraints	4
10 lowest-energy structures	
NOE constraint violations	0 (>0.5 Å)
dihedral angle constraint violations	0 (>30°)
rmsd from average (all coordinates)	0.97 Å
pairwise rmsd (all coordinates)	1.35 Å
rmsd from average (residue 1)	0.84 Å
rmsd form average (residue 2)	0.55 Å
rmsd from average (residue 3)	0.46 Å
rmsd from average (residue 4)	0.46 Å
rmsd from average (residue 5)	0.67 Å
rmsd from average (residue 6)	1.95 Å
energy	−395 ± 5 kcal/mol

took the bulk of the time required for solving the structure. The refined structure shows good agreement between experimental and back-calculated NOESY spectra over the entire ppm range (Figure 3). Furthermore, all low-energy structures are of the same fold and free of violations of constraints (Figure 4).

The duplex is slightly bent, and the nucleobases of the T1 residues rest on top of the oxolinic acid residues with the hydrophobic methyl group toward the flat surface of the quinolone ring system and partial packing of the methyl group against the ethyl side chain of the oxolinic acid. (Figure 5). Together, the oxolinic acid residue and the deoxyadenosine residue form a cap that covers the G2:C5 base pair (Figure 6). The disruption of what would otherwise have been the T1:A6 base pair is such that both the riboses and the nucleobases are far displaced from a position that would allow them to interact even in a dynamic equilibrium. Still, the structure is tightly packed, with the exception of the T1, which makes limited contact with the rest of the folded structure. Due to the placement of the 3′-terminal deoxyadenosine residue in the minor groove and the absence of the T:A base pair, the duplex is more globular in structure than is typical for a DNA duplex. The more rapid tumbling of a globular structure compared to that of a fully extended helix may explain the very sharp signals (half-height peak widths between 3.1 and 4.0 Hz) observed in the one-dimensional ^{1}H NMR spectrum of (**1oa**)$_2$ (Figure S11, Supporting Information). The structure also helps to explain why the non-annulated ring of pipemidic acid, norfloxacin, and ofloxacin does not induce a steric clash. If their quinolone core is positioned like that of oxolinic acid, the piperazine will

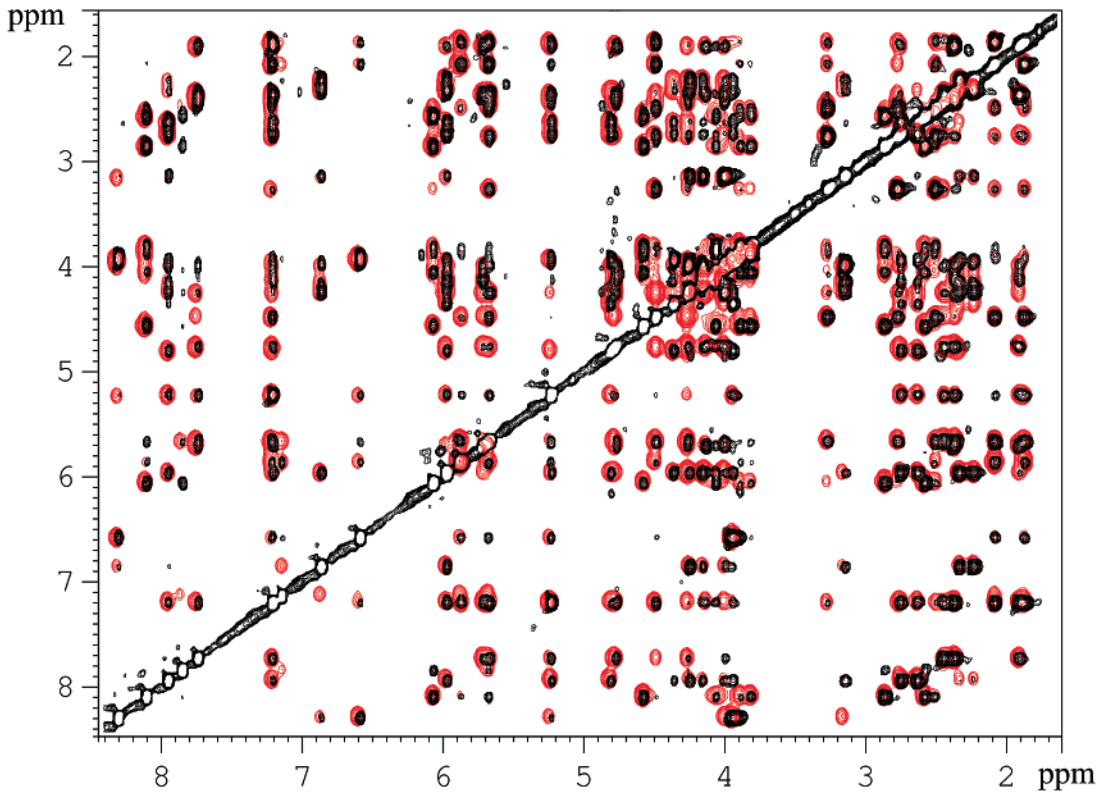

Figure 3. Overlay of experimental (black) and back-calculated (red) NOESY spectrum of (**1oa**)$_2$ in D_2O. The experimental spectrum was acquired at 600 MHz, 283 K, 10 mM phosphate buffer, 150 mM NaCl, with a mixing time of 300 ms. The back-calculated spectrum was generated in GIFA[42] using the two-spin approximation and cross-peak intensities calculated in X-PLOR[40] from one of the violation-free low-energy structures shown in Figure 4.

Figure 4. Overlay of the 10 violation-free structures of (**1oa**)$_2$ of lowest energy, as obtained from restraint molecular dynamics calculations in CNS.[15] The graphic was generated with VMD.[44] Coloring code: hydrogen, white; carbon, green; nitrogen, blue; oxygen, red; phosphate, yellow.

protrude into the major groove, where their protonated secondary amine may form an ion pair with the phosphodiester anion linking C5 and A6, resulting in the extra stabilizing effect noted at low salt concentration.

Since the folded structure of oxolinic acid-bearing (oa-T*GCGCA)$_2$ is unusual and features only four base pairs, a thermodynamic analysis of the duplex-to-single strands transition was performed, together with that of control duplex (**2**)$_2$. The results from this analysis are presented in Table 6 for 1 M salt concentration and Table S4 (Supporting Information) for 150 mM salt concentration. It can be discerned that the quinolone-bearing duplex is entropically more costly to form, but enthalpically more stable than the control duplex. Therefore, the enhanced stability of the duplex is not due to more extensive preorganization of the single strands, but rather direct enthalpic gains, possibly based largely on additional stacking enthalpy between the quinolone and the G:C base pair. By the same argument, the higher entropic penalty that prevents further duplex stabilization indicates that more substantial folding and thus ordering occur when **1oa** forms a duplex.

Discussion

Oligonucleotides with a quinolone cap at the 5′-terminus were initially synthesized with the goal of stabilizing the terminal T:A base pair through stacking interactions. The assay employed screened for duplex stability, assuming that interactions from the disruption of base pairs will not stabilize duplexes. While the screen was successful, the structural assumption was not. Even though the melting points of the duplex (**1oa**)$_2$, is high, it has no more than four intact base pairs of the sequence 5′-GCGC-3′. The calculated melting point for an unmodified tetramer duplex of this sequence is 2.8 °C at 1 μM strand concentration and 1 M salt concentration.[16] At 5 μM strand concentration, the calculated melting point is 10.5 °C. For (**1oa**)$_2$,

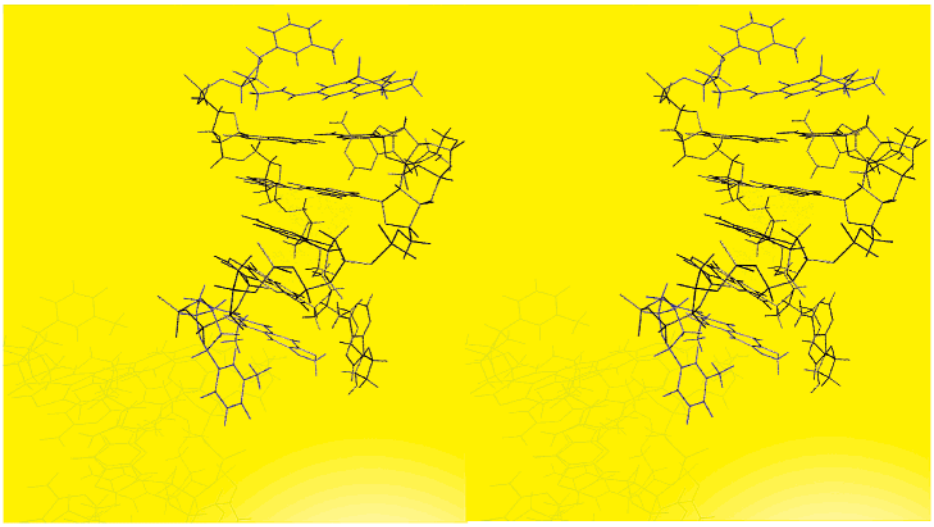

Figure 5. Stereoimage of a low-energy structure of (**1oa**)$_2$, selected from one of the structures shown in Figure 4. View onto the major groove of the core duplex. A shadow of the structure is seen in the lower left corner of each image as the result of the rendering process, employed to improve the stereo effect.

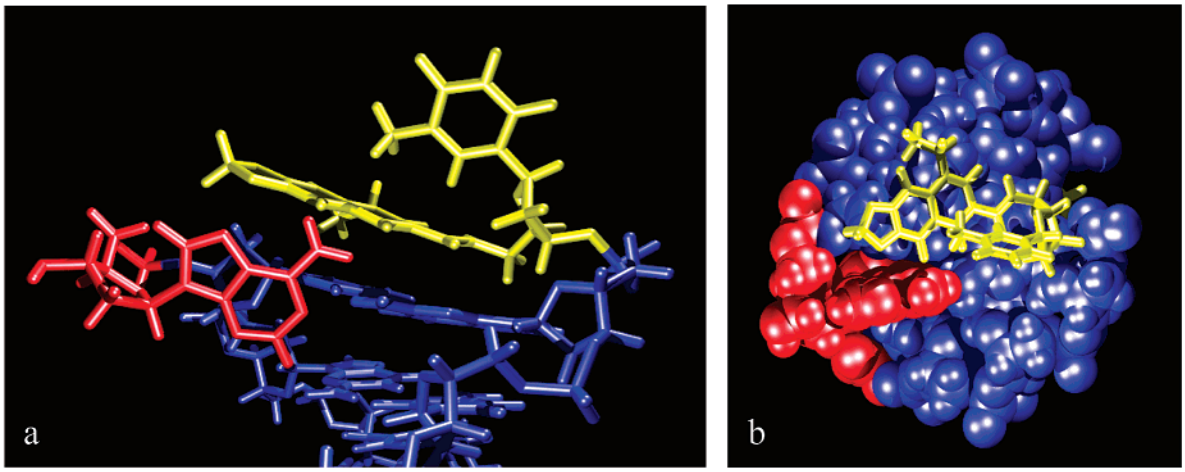

Figure 6. Structural images of the fold of (**1oa**)$_2$ at the terminus. (a) View from the minor groove, (b) view along the helix axis. The structure displayed was chosen from those shown in Figure 4. Color code: T1 and oxolinic acid residue, yellow; A6, red; residues of the core duplex, blue.

Table 6. Thermodynamic Parameters for Duplex Dissociation at 1 M Salt,[a] Derived from Fits to the UV Melting Data Using the Program Meltwin.[43]

duplex	$\Delta H°$ (kcal/mol)	$\Delta S°$ (cal/mol K)	$\Delta G°$ (kcal/mol)
$(TGCGCA)_2$ (**2**)$_2$	42.8	114	7.4
(oa-T*GCGCA)$_2$ (**1oa**)$_2$	54.6	140	11.3

[a] Melting experiments were performed at 3.1 ± 0.3 μM strand concentration and 1 M NH_4OAc concentration, pH 7.0.

59.5 °C was measured at 3.1 μM strand concentration, giving a calculated melting point increase of 49 °C induced by the caps (24.5 °C per cap). Therefore, the composite cap formed by the residues of oxolinic acid, thymidine, and the displaced adenosine is more effective than the most stabilizing 5′-cap found thus far (a steroid), even though the latter stabilizes duplexes via intact terminal base pairs.[9,17] Since oxolinic acid, as a moiety of 244 g/mol residue weight induces base-pair disruption without net energetic penalty, our results reinforce arguments that nature did not evolve DNA base pairs toward maximum stability.[18] The cause for this apparent lack of stability is probably that DNA strands have to be separated for replication, transcription, and repair.

It should be kept in mind, however, that the ease of giving up a base pair in favor of stacking interactions with a heterocycle and groove binding of one of the displaced residues will certainly depend on the nature of the base pair. It should be easier to disrupt a T:A base pair than a C:G base pair. Our results with quinolones appended to terminal deoxycytidine residues suggest, however, that C:G base pairs are apparently not immune to disruption. In a recent combinatorial study,[9] aimed at finding caps for terminal C:G base pairs, six quinolones (nalidixic acid, oxolinic acid, cinoxacin, lomefloxacin, ofloxacin, and pipemidic acid) were found to stabilize duplexes. Melting points for R−C*GGTTGAC in duplex with GTCAACCG, where R is the residue of oxolinic acid, ofloxacin, cinoxacin, lomefloxacin, or pipemidic acid, were 3.9−4.8 °C higher at 10 mM

(16) Melting points were calculated using software developed in-house (Tetzlaff, C. N. Ph.D. Thesis, Tufts University, 2001), based on parameters reported in: SantaLucia, J.; Allawi, H. T.; Senevirante, P. A. *Biochemistry* **1996**, *35*, 3555−3562.

(17) Bleczinski, C. F.; Richert, C. *J. Am. Chem. Soc.* **1999**, *121*, 10889−10894. For related work with sterols, see: Letsinger, R. L.; Chaturvedi, S. K.; Farooqui, F.; Salunkhe, M. *J. Am. Chem. Soc.* **1993**, *115*, 7535−7536.

(18) Beier, M.; Reck, F.; Wagner, T.; Krishnamurthy, R.; Eschenmoser, A. *Science* **1999**, *283*, 699−703.

salt concentration and 1.9−5.9 °C higher at 1 M salt concentration, compared to the duplex where R is an acetyl group.[9] Probably, the smaller ΔT_m's measured for these C:G-terminated duplexes (compared to those with T and A as terminal residues, Table 2) are the result of the more difficult-to-disrupt C:G base pairs.

But, the complex between the composite cap of oa, T and A and the termini of duplexes is not only very stable, it is also fairly specific. Mismatches in what it caps as the true terminal base pair are not tolerated well. At the outset of our study on caps for DNA termini that prevent fraying and improve base-pair fidelity, we defined the goal of finding caps that induce melting point depressions of >15 °C per mismatch. This value is similar to what can be achieved at the central positions of octamer duplexes and is usually sufficient to give <5% false positive signal in hybridization experiments on DNA chips, assuming that the transition breadth (cooperativity) of the corresponding melting transitions is that of typical short duplexes on a flat surface.[19] With the oa-T*/A cap, the three possible mismatches for the now terminal base pair all induce a melting point depression of ≥15.7 °C (Table 2). Therefore, the composite cap achieves the goal defined above and provides a blueprint for the design of caps made of a single molecular moiety.

How then is the increase in base-pairing fidelity achieved by the composite cap? The structure of (**1oa**)$_2$ indicates that the oa-T*/A cap binds exclusively on the top of the now terminal G:C base pair and in the minor groove. It is interesting that some polymerases, that is, enzymes that have to ensure exquisite base-pairing fidelity, also contact the NTP−primer−template complex from the minor groove and the top of the terminal base pair.[20] The major groove, however, is not bound in the active site of these polymerases, even though molecular dynamics seem to suggest that opening of base pairs into the major groove is the main motion underlying duplex breathing.[21] Therefore, L-shaped ligands contacting the flat face of the terminal base pair and the minor groove may provide the contacts required for a high fidelity base-pairing environment. For T:A base pairs, these may be constructed by extending the known steroid caps[17] by a minor groove binding moiety. Work along these lines is in progress in these laboratories.

The derivatives of **1** studied (Table 1) demonstrate that the capping effect is a general phenomenon, in that all quinolones tested give a stabilizing effect. Oxolinic acid does not have readily ionizable groups that could form ions pairs with phosphodiester anions, nor are there any detectable hydrogen bonds to the DNA in the structure of (**1oa**)$_2$. Further, the effect does not require a specific residue to which the quinolone is appended.[9] Nor is a direct link between quinolone and the 5′-terminus required for a stabilizing effect, though such a link does favor a tight complex. The strength of the interactions is surprising, given that oxolinic acid boasts but two aromatic rings and three rings total.[22] Why, then, are these stacking interactions stronger than those observed with other ring systems of similar size?[8,9] Apparently, dipoles and quadrupoles of the ring systems involved are complementary and provide forces that add to the van der Waals forces and hydrophobic effect expected for the interactions of oxolinic acid and the DNA.

Quinolones are, of course, known to bind to double-stranded DNA. But their exact binding mode has remained elusive. While studying the binding of norfloxacin, a fluoroquinolone, to DNA with a number of spectroscopic techniques, Kim, Norden, and collaborators detected a "near-perpendicular orientation of the norfloxacin chromophore plane" to the DNA helix axis of calf thymus DNA.[23] Still, they were able to exclude both classical intercalation, classical groove, and classical surface binding modes. In the structure of (**1oa**)$_2$, oxolinic acid is found in a position roughly perpendicular to the helix axis. If a substantial number of termini existed in the preparation, or if partial denaturation occurred while binding was studied, structures similar to the one observed in our covalent hybrids may have been detected by those authors.

Given the disrupted base pair, it is tempting to discuss the current results in light of the effect of quinolones as gyrase inhibitors. A detailed model for the ternary complex of quinolones, DNA, and gyrase was developed by Shen and collaborators in 1989.[24] In this model, quinolones were proposed to bind to the DNA−gyrase complex after the cleavage of the DNA, such that the drugs interact directly with each other, either through stacking or through "zipper-like" packing between side chains of intercalated heterocyclic rings. For quinolones with antineoplastic activity, that is, inhibitors of mammalian topoisomerases II, a model was proposed by Hurley and co-workers, in which quinolones also interact directly with each other and their 2:2 complexes with DNA are mediated by Mg^{2+} ions.[25] The most recent model for the quinolone−DNA−gyrase complex, based on work with gyrase mutants and kinetic and crystallographic data,[3a,5,26] was proposed by Maxwell and collaborators.[7] In this model, two quinolone molecules bind to the gyrase-bound DNA at sites four nucleotides apart, without interacting with each other. The interaction with the DNA is believed to involve stacking with bases and to be favored by distortion of the DNA helix by the enzyme.[7] Other authors also cite perturbations in the DNA structure in quinolone−DNA complexes.[27]

Oxolinic acid-induced DNA cleavage by gyrase is known to occur preferentially at a phosphodiester linkage with a 5′-thymidine and a 3′-deoxyguanosine residue,[28] that is, between the very nucleotides where the disruption of the duplex is found in our structure. If the current structure has any relevance for the quinolone−DNA complex that blocks the gyrase reaction cycle (and indirectly transcription), it supports the most recent

(19) Peterlinz, K. A.; Georgiadis, R. M. *J. Am. Chem. Soc.* **1997**, *119*, 3401−3402.
(20) (a) Doublie, S.; Tabor, S.; Long, A. M.; Richardson, C. C.; Ellenberger, T. *Nature* **1998** *391*, 251−258. (b) Huang, H.; Chopra, R.; Verdine, G. L. Harrison, S. C. *Science* **1998**, *282*, 1669−1675.
(21) See e.g.: Cubero, E.; Sherer, E. C.; Luque, F. J.; Orozco, M.; Laughton, C. A. *J. Am. Chem. Soc.* **1999**, *121*, 8653−8654 and references therein.
(22) Studies where an abasic residue was used to provide a site where a nucleobase analogue can stack on a base pair suggest that tetracyclic compounds produce a good fit: (a) Guckian, K. M.; Schweitzer, B. A.; Ren, R. X. F.; Sheils, C. J.; Paris, P. L.; Tahmassebi, D. C.; Kool, E. T. *J. Am. Chem. Soc.* **1996**, *118*, 8182−8183. (b) Matray, T. J.; Kool, E. T. *J. Am. Chem. Soc.* **1998**, *120*, 6191−6192. (c) Guckian, K. M.; Schweitzer, B. A.; Ren, R. X.-F.; Sheils, C. J.; Tahmassebi, D. C.; Kool, E. T. *J. Am. Chem. Soc.* **2000**, *122*, 2213−2222.
(23) Son, G. S.; Yeo, J.-A.; Kim, M.-S.; Kim, S. K.; Holmen, A.; Akerman, B.; Norden, B. *J. Am. Chem. Soc.* **1998**, *120*, 6451−6457.
(24) Shen, L. L.; Mitschler, L. A.; Sharma, P. N.; O'Donnell, T. J.; Chu, D. W. T.; Cooper, C. S.; Rosen, T.; Pernet, A. G. *Biochemistry* **1989**, *28*, 3886−3894.
(25) Fan, J.-Y.; Sun, D.; Yu, H.; Kerwin, S. M.; Hurley, L. H., *J. Med. Chem.* **1995**, *38*, 408−424.
(26) (a) Kampranis, S. C.; Maxwell, A. *J. Biol. Chem.* **1998**, *273*, 22606−22614. (b) Kampranis, S. C.; Maxwell, A. *J. Biol. Chem.* **1998**, *273*, 22615−22626.
(27) Marians, K. J.; Hiasa, H. *J. Biol. Chem.* **1997**, *272*, 9401−9409.
(28) Lockshon, D.; Morris, D. R. *J. Mol. Biol.* **1985**, *181*, 63−74.

structural proposal.[7] There are no direct interactions between the quinolone molecules, and the NMR data do not suggest aggregation or lamellar stacking of duplexes via the quinolones. In fact, the resonances are very sharp, possibly because the overall structure is more globular than an undisturbed DNA duplex of similar molecular weight. There are stacking interactions between the quinolones and the nucleobases, however. Further, the structure of the DNA is disturbed, as proposed by Maxwell and collaborators.[7] The way in which the nucleotides of the T:A base pair are arranged in (**1oa**)$_2$ does indeed suggest how resealing of DNA cleaved by the gyrase could be prevented by the quinolones. The drugs not only drive apart the nucleotides of the terminal base pairs, they also force the adenosine residues into the minor groove, such that their 3′-hydroxyl group will not be available for resealing. Despite the disruption, the formation of the intraduplex DNA−quinolone complexes is very favorable energetically.

Conclusions

Quinolone residues, when covalently bonded to 5′-terminal pyrimidine residues of short oligonucleotides, stabilize duplexes against thermal denaturation. At least for the oxolinic acid residue, whose interactions with DNA were studied in detail, the stabilizing effect enhances the base-pairing fidelity of the penultimate nucleotide that it stacks upon. The quinolone achieves its stabilizing effect despite disruption of the terminal T:A base pair. Circumstantial evidence, such as that oxolinic acid is known to induce gyrase cleavage preferentially at T−G steps, that norfloxacin has been shown to bind to duplex DNA with a similar angle to the helix axis as seen in the NMR structure, and that the disruption of the terminal base pair is in line with inhibition of resealing, points toward a relevance for the biological activity of quinolones.

Experimental Section

General. Anhydrous solvents were purchased over molecular sieves and were used without further modification. Reagents were the best available grade from Acros (Geel, Belgium), Aldrich/Fluka/Sigma (Deisenhofen, Germany), or Advanced ChemTech (Louisville, KY) and were used without purification. Quinolones were from Aldrich (nalidixic acid) or Sigma (oxolinic acid, cinoxacin, pipemidic acid, norfloxacin, and ofloxacin) (both Deisenhofen, Germany), and Fmoc-Gly-OH was from Acros (Geel, Belgium) and were used as received. DNA synthesis reagents were from Proligo (Hamburg, Germany). The 5′-monomethoxytrityl-proteted 5′-amino-5′-deoxythymidine phosphoroamidite[30] was synthesized as described.[29] The Fmoc-protected building blocks of norfloxacin and pipemidic acid required for coupling to the amino-terminal DNA were prepared in one-step reactions with Fmoc-OSu as described earlier for pipemidic acid.[9] Oligonucleotides were purified by HPLC on a 250 mm × 4.6 mm Macherey-Nagel Nucleosil C4 column, using a gradient of CH_3CN (solvent B) in 0.1 M triethylammonium acetate, pH 7, and detection at 260 nm. Yields of DNA hybrids are based on the intensity of product peaks in the HPLC traces of the crude products. The integration was not corrected for the absorbance caused by the solvent front. MALDI-TOF spectra were recorded on a Bruker BIFLEX III spectrometer in negative, linear mode. The matrix mixtures for oligonucleotides were prepared from 2,4,6-trihydroxyacetophenone (THAP, 0.3 M in ethanol) and diammonium citrate (0.1 M in water) (2:1, v/v). Calculated masses are average masses; *m*/*z* found are those for the pseudomolecular ions ($[M - H]^-$), detected as the maximum of the unresolved isotope pattern. The accuracy of mass determination with the external calibration used is ca. ±0.1%, that is, ±2 Da at *m*/*z* 2000. NMR spectra were acquired on Bruker 600 DPX spectrometers. DNA sequences are given 5′-to-3′ terminus; T* denotes a 5′-amino-5′-deoxythymidine residue.

Synthesis of Oligonucleotides. The unmodified DNA portion of the oligodeoxyribonucleotides was synthesized on an ABI 380 DNA synthesizer according to the manufacturer's recommendations, employing the 5′-MMT-protected 3′-phosphoramidite of 5′-amino-5′-deoxythymidine[29] in the last coupling step under standard coupling conditions. The strands were synthesized on a 1.0 μmol scale, except for the NMR samples, which were synthesized on a 10 μmol scale. After removal of the MMT group under standard deblocking conditions, quinolones were coupled to the amino groups thus liberated under conditions reported earlier.[8,19,31] Briefly, a mixture of the carboxylic acid (100 μmol), HBTU (34.1 mg, 90 μmol), and HOBT (15.3 mg, 100 μmol) was dissolved in DMF (600 μL), treated with DIEA (40 μL, 234 μmol), vortexed, and injected into a column containing controlled pore glass (CPG) bearing the amino-terminal DNA (3 mg, with approximately 0.1 μmol DNA on its surface). As mentioned in the General section, norfloxacin and pipemidic acid were coupled with the secondary amine of the piperazine ring protected with a fluorenylmethoxycarbonyl protecting group.[9] Quinolones not fully soluble in the coupling mixture were reacted as a slurry, the solid being excluded from the CPG by the fritte closing off the column. After 40 min, the CPG was washed with DMF (2 × 1.5 mL) and MeOH (2 × 1.5 mL), followed by drying at 0.1 Torr. For quinolone−DNA hybrid **1oag**, coupling of the oxolinic acid was preceded by coupling of Fmoc-Gly-OH and deprotection with piperidine/DMF (1:4) as previously described.[31] The CPG bearing the fully assembled oligomer was transferred to a polypropylene reaction vessel and deprotected with ammonium hydroxide at room temperature for 16 h. Solutions of crude oligonucleotides were lyophilized, redissolved in water, and subjected to HPLC purification.

oa-T*GCGCA (1oa): yield 53%; HPLC gradient of 0% B for 3 min, in 35 min to 25% B, in 3 min to 80% B, t_R = 27.1 min. MALDI-TOF MS *m*/*z* for $C_{71}H_{83}N_{25}O_{37}P_5$ $[M - H]^-$: calculated 2033.5, found 2033.2.

na-T*GCGCA (1na): yield 60%; HPLC gradient of 0% B for 3 min, in 35 min to 25% B, in 3 min to 80% B, t_R = 27.2 min. MALDI-TOF MS *m*/*z* for $C_{70}H_{84}N_{26}O_{35}P_5$ $[M - H]^-$: calculated 2004.5, found 2004.4.

ci-T*GCGCA (1ci): yield 55%; HPLC gradient of 0% B for 3 min, in 35 min to 25% B, in 3 min to 80% B, t_R = 26.2 min. MALDI-TOF MS *m*/*z* for $C_{70}H_{82}N_{26}O_{37}P_5$ $[M - H]^-$: calculated 2034.4, found 2033.1.

pi-T*GCGCA (1pi): yield 62%; HPLC gradient of 0% B for 3 min, in 35 min to 25% B, in 3 min to 80% B, t_R = 26.9

(29) Tetzlaff, C. N.; Schwope, I.; Bleczinski, C. F.; Steinberg, J. A.; Richert, C. *Tetrahedron Lett.* **1998**, *39*, 4215−4218.
(30) Bannwarth, W. *Helv. Chim. Acta* **1988**, *71*, 1517−1527.
(31) Schwope, I.; Bleczinski, C. F.; Richert, C. *J. Org. Chem.* **1999**, *64*, 4749−4761.

min. MALDI-TOF MS *m*/*z* for $C_{72}H_{89}N_{29}O_{35}P_5$ [M − H]$^-$: calculated 2075.5, found 2074.6.

nr-T*GCGCA (1nr): yield 60%; HPLC gradient of 0% B for 3 min, in 35 min to 25% B, in 3 min to 80% B, t_R = 28.7 min. MALDI-TOF MS *m*/*z* for $C_{74}H_{90}FN_{27}O_{35}P_5$ [M − H]$^-$: calculated 2091.6, found 2090.4.

of-T*GCGCA (1ofI/II):[32] yield 18/22%; HPLC gradient of 0% B for 3 min, in 35 min to 25% B, in 3 min to 80% B, t_R = 28.7/29.7 min. MALDI-TOF MS *m*/*z* for $C_{76}H_{92}FN_{27}O_{36}P_5$ [M − H]$^-$: calculated 2133.6, found 2132.6/2132.7.

oag-T*GCGCA (1oag): yield 36%; HPLC gradient of 0% B for 5 min, in 30 min to 30% B, in 10 min to 100% B, t_R = 27.2 min. MALDI-TOF MS *m*/*z* for $C_{73}H_{87}N_{26}O_{38}P_5$ [M − H]$^-$: calculated 2090.3, found 2088.5.

oa-T*GCGCAACT (3oa): yield 42%; HPLC gradient of 0% B for 3 min, in 35 min to 28% B, in 10 min to 100% B, t_R = 25.6 min. MALDI-TOF MS *m*/*z* for $C_{100}H_{121}N_{35}O_{55}P_8$ [M − H]$^-$: calculated 2939.6, found 2939.9.

oa-T*GGTTGAC (5oa): yield 42%; HPLC gradient of 0% B for 5 min, in 30 min to 30% B, in 10 min to 100% B, t_R = 27.4 min. MALDI-TOF MS *m*/*z* for $C_{92}H_{111}N_{31}O_{51}P_7$ [M − H]$^-$: calculated 2681.5, found 2680.9.

oa-Lys-T*GGTTGAC (5oak): employed for melting curve study whose results are presented in Table S5 (Supporting Information); prepared using Fmoc-Lys(TFA)-OH as amino acid building block and the protocol of ref 31. Yield 48%; HPLC gradient of 0% B for 5 min, in 30 min to 30% B, in 10 min to 100% B, t_R = 25.4 min. MALDI-TOF MS *m*/*z* for $C_{98}H_{123}N_{33}O_{52}P_7$ [M − H]$^-$: calculated 2810.6, found 2811.4.

UV Melting Experiments. UV melting experiments were performed with a Perkin-Elmer Lambda 10 spectrophotometer at 260 nm and 1 cm path length at heating or cooling rates of 1 °C/min. Extinction coefficients of quinolone−DNA hybrids were calculated as the sum of the extinction coefficients of the DNA portion and the following ϵ_{260} of the quinolones, nalidixic acid (20300 M^{-1} cm^{-1}), oxolinic acid (41800 M^{-1} cm^{-1}), cinnoxacin (24100 M^{-1} cm^{-1}), ofloxacin (6500 M^{-1} cm^{-1}), norfloxacin (9500 M^{-1} cm^{-1}), pipemidic acid (20700 M^{-1} cm^{-1}). Solutions with salt concentrations of 150 mM and 1 M were produced by addition of aliquots of a 5 M solution of NH_4-OAc, and the strand concentrations are uncorrected for the dilution effect. Prior to acquisition of the melting curves, duplexes were annealed by heating to 90 °C, followed by cooling to 5 °C at a rate of 2 °C/min. Melting temperatures were determined with UV Winlab 2.0 and are averages of the extrema of the first derivative of the 91-point smoothed curves from heating and cooling experiments. Hyperchromicities were determined by calculating the ΔE_{260} between high- and low-temperature baseline and dividing by the E_{260} of the low-temperature baseline. Thermodynamic data were calculated using Meltwin,[33] based on melting curve data (one extinction value per °C, so as to allow fitting over a sufficient temperature range). Meltwin was kindly provided by Drs. McDowell and Turner.

NMR Spectroscopy. HPLC-purified **1oa** was lyophilized six times from 10% ammonium hydroxide to remove residual triethylamine and, in the case of D_2O samples, twice from D_2O. Samples were prepared by dissolving the residue either in D_2O (99.999% D), or in H_2O/D_2O (85:15) containing 150 mM NaCl and 10 mM phosphate buffer (KH_2PO_4/K_2HPO_4) at pH 7.0 (uncorrected for deuterium effect). Sample of 185−230 μL were prepared in NMR microtubes susceptibility matched to D_2O (Shigemi Co., Tokyo, Japan). Strand concentrations were between 2 and 10 mM. Spectra were recorded on a Bruker DPX 600 spectrometer at the Francis Bitter Magnet Laboratory, M.I.T. at 283 K and spectral widths of 6000 Hz (D_2O samples) or 12000 Hz (H_2O/D_2O samples). Suppression of the excess solvent peak was achieved via presaturation during the recycle delay (D_2O samples) or via the WATERGATE gradient pulse sequence[34] (H_2O/D_2O samples). NOESY[35] spectra were acquired at mixing times of 75, 150, 225, and 300 ms. DQF-COSY[36] and TOCSY[37] (spin lock time 60 ms) were recorded to aid signal assignment. For all spectra, 256 or 400 increments were recorded in F1 with spectral sizes of 2K or 4K in F2 and 32 scans per increment. Spectra were processed using XWINNMR (Bruker Instruments), including zero filling to 1K data points in F1, apodization with Gaussian and exponential functions, and automatic baseline correction. Build-up curves for representative cross-peaks in the D_2O NOESY spectra at different mixing times showed that up to 300 ms the intensity of the cross-peaks rises with little loss due to spin diffusion.

Resonance Assignments and Generation of Constraints. Peak assignment for H1′- and H6/8-protons of the nucleotides was based on an established strategy.[14] The cross-peak from H1′−T1 to H8−G2 was difficult to pursue for further assignment because of an overlap between H1′−T1 and H1′−G2. Sequential assignment from the 3′-terminus and deletion analysis for the singlets in the aromatic region were therefore included in the analysis. On the basis of the H1′-resonances of all nucleotides, chemical shifts of ribose protons were assigned via DQF-COSY and TOCSY cross-peaks, together with confirmation via NOESY cross-peaks for the core tetramer, where an intact Watson−Crick duplex was identified early on. H5's of cytidine residues and H2 of A6 were identified via DQF-COSY cross-peaks to their vicinal H6's and a NOESY cross-peak to H1′, respectively. The chemical shift of the methyl group of T1 (CH_3-7) was assigned on the basis of the NOESY cross-peak to H6 of that residue. For the oxolinic acid residue, the characteristic spin system of the ethyl side chain provided a starting point whose NOESY cross-peaks identified neighboring aromatic protons of the quinolone. A NOESY cross-peak from H8 to the two diastereotopic methylene protons of the dioxolane ring then provided a step to assigning H5 via the equivalent connectivity. All non-exchangeable protons, except H5′/H5″ of guanosine and cytidine residues were thus assigned.

Distance constraints were generated from cross-peaks in a NOESY spectrum of a D_2O sample with a mixing time of 300 ms. Integration in XWINNMR produced intensities that were used to define a calibration function with the aid of cross-peaks between protons with known distances, such as H5 and H6 of cytidines. On the basis of this calibration, cross-peak intensities

(32) It is known that the two enantiomers of ofloxacin have different activities against DNA gyrase: Morrissey, I.; Hoshino, K.; Sato, K.; Yoshida, A.; Hayakawa, I.; Bures, M. G.; Shen, L. L. *Antimicrob. Agents Chemother.* **1996**, *40*, 1775−1784.

(33) McDowell, J. A.; Turner, D. H. *Biochemistry* **1996**, *35*, 14077−14089.

(34) Sklenar, V.; Piotto, M.; Leppik, R.; Saudek, V. *J. Magn. Reson., Ser. A* **1993**, *102*, 241−245.

(35) Kumar, A.; Ernst, R. R.; Wüthrich, K. *Biochem. Biophys. Res. Commun.* **1980**, *95*, 1−6.

(36) Piantini, U.; Sørensen, O. W.; Ernst, R. R. *J. Am. Chem. Soc.* **1982**, *104*, 6800−6801.

(37) Bax, A.; Davis, D. G. *J. Magn. Reson.* **1985**, *65*, 355−360.

were converted into distances and provided with error margins of between ±0.5 and ±1.5 Å, depending on the quality and intensity of the cross-peak. Cross-peaks that were partially overlapped or obtained from spectra in H_2O/D_2O were qualitatively classified as weak (4.5 Å), medium (3.5 Å), or strong (2.5 Å) and entered with error margins of ±1.0 A. Constraints from and to methylene protons that were not assigned stereospecifically and from methyl groups were entered using the pseudoatom approach; the corresponding distance constraints were provided with error margins of up to ±2 Å. Trivial distance constraints, for example those resulting from geminal protons, were not entered, as their relative positions are well-defined by the force-field parameters.

All H1′-protons of the nucleotides showed intraresidue NOESY cross-peaks characteristic for B-form DNA. Further, they appeared as triplets with ^3J coupling constants in the range of 6.5−7.3 Hz, as expected for the South or 2′-endo conformation. Further, DQF-COSY cross-peak patterns between H1's and H2′/H2′'s were similar to those predicted for B-form DNA.[38] On the basis of this information and the low-field resonances for NH1 of G2 and G4, constraints for backbone dihedral angles were generated for the core tetramer (G2−C3−G4−C5) using B-from angles from the literature[39] and initial error margins of ±50 °, reduced to ±20 ° and ±30 ° during refinement. Further, gentle (pscale 15) base-pair planarity and hydrogen-bonding constraints were used for the Watson−Crick base pairs of the central tetramer duplex. Hydrogen-bond constraints used distances provided with X-PLOR[40] and had error margins of ±0.1 Å.

Structure Generation. Generation of topology and parameter files were performed in X-PLOR, version 3.851.[40] Restrained molecular dynamics calculations were carried out in CNS,[15] version 1.0 on LINUX or IRIX platforms, using the torsion angle molecular dynamics option. Parameters used for calculations were identical to those employed in earlier work.[41] A total of 30 constraints to and from the oxolinic acid residues were employed. Table 5 provides an overview over all constraints used. Refinement was based chiefly on optimizing the agreement between back-calculated and experimental NOESY spectra. Back-calculation of expected cross-peaks and their intensities were performed in X-PLOR, using a representative structure of low energy and without constraint violations. Back-calculated spectra were generated from the cross-peak list thus obtained with the rigid body two-spin approximation option in GIFA.[42] In the NOESY overlay for the refined structure (Figure 3), of 197 cross-peaks above the diagonal, 10 experimental peaks were unmatched in the back-calculated spectrum, and five of those of the back-calculated spectrum were unmatched by experimental spectrum. The remaining unmatched peaks are scattered over a number of resonances and are believed to reflect limitations of the simplified model employed for back-calculations, as well as instrumental artifacts in the experimental spectrum and incomplete assignments. Considering that some experimental cross-peaks appear only below the diagonal, the agreement is better than 95%. Statistics on the 10 lowest-energy structures that were violation-free are given in Table 5.

Acknowledgment. The authors would like to thank Drs. Ina Schwope and Colleen Bleczinski for synthetic work leading to NMR samples of **1oa**, Dr. Susan Pochapsky for help with the acquisition and interpretation of NMR spectra, Dr. Luke Rice for help with molecular dynamics, Karsten Siegmund and Dr. Charles Tetzlaff for help with computer issues, and Drs. C. Steinbeck and S. Maheshwary for helpful discussions. This work was supported by the NIH (Grant GM54783 to C.R.), the Deutsche Forschungsgemeinschaft (Grant No. RI 1063/1 to C.R.), and Fonds der Chemischen Industrie (Account 164431). The Center for Magnetic Resonance at the Francis Bitter Magnet Laboratory was supported by Grant No. RR00995, from the National Center for Research Resources at the NIH. J.T. is a recipient of a predoctoral fellowship from The State of Baden-Württemberg.

Supporting Information Available: MALDI-TOF mass spectra of modified oligonucleotides, 1D NMR spectra of **1oa** at different temperatures, expansions of NOESY NMR spectrum of $(\mathbf{1oa})_2$ with key assignments and key cross-peaks highlighted, structural image of $(\mathbf{1oa})_2$ with distance constraints shown, image with stacking interactions between oa and the G2:C5 base pair, chemical shifts for protons of $(\mathbf{1oa})_2$, list of predicted and experimental NOESY cross-peaks to and from the oxolinic acid residue, comparison of chemical shifts of non-exchangeable aromatic nucleobase protons of $(\mathbf{1oa})_2$ with those of control duplex $(TGCGCAC)_2$, enthalpy and entropy of duplex dissociation for duplexes listed in Table 1, and UV melting points for duplexes of oa-Lys-T*GGTTGAC and GTCAACCA or GTCAACCA (PDF). This material is available free of charge via the Internet at http://pubs.acs.org. Coordinates of $(1oa)_2$ have been deposited with the Protein Data Bank, entry code 1KSE. They are available free of charge at http://www.resb.org/pdb/.

JA0125117

(38) Wijmenga, S. S.; Mooren, M. M. W.; Hilbers, C. W. In *NMR of Macromolecules, A Practical Approach*; Roberts, G. C. K., Ed.; Oxford University Press: Oxford, UK, 1993; pp 217−288.
(39) Saenger, W. *Principles of Nucleic Acid Structure*; Springer: New York, 1984.
(40) *X-PLOR*, version 3.1; Brünger, A. T. X-PLOR Manual, Yale University Press: Yale University, New Haven, CT, 1992.
(41) Ho, W. C.; Steinbeck, C.; Richert, C. *Biochemistry* **1999**, *38*, 12597−12606.
(42) Delsuc, M. A. In *Maximum Entropy and Bayesian Methods*; Skilling, J., Ed.; Kluwer Academic: Dordrecht, The Netherlands, 1989; pp 285−290.
(43) McDowell, J. A.; Turner, D. H. *Biochemistry* **1996**, *35*, 14077−14089.
(44) Humphrey, W.; Dalke, A.; Schulten, K. *J. Mol. Graphics* **1996**, *14*, 33−38.